# Pushover Analysis of Steel Frames with Buckling Restrained Braces focusing Slab-Composite Effect

**Y. Ohko, & T. Yamashita**
*Kogakuin University, Tokyo, Japan*

**SUMMARY:**
This paper proposes a scheme to estimate the axial force of beams in the steel multi-story buildings in which Buckling Restrained Braces (BRB) are used. In the analysis using rigid-floor model, beam axial force is often ignored. But in actual, beams connected to BRBs are subjected to axial force, thus the steel beams should be designed for combination of axial force and bending. In this paper, a simple method to estimate axial force in the beams to which BRBs are connected, is demonstrated and its accuracy is verified using FE models.

*Keywords: Composite beam, Floor slab, Buckling Restrained Brace, Axial force, Inertia force*

## 1. INTRODUCTION

Recently, use of BRB (Buckling Restrained Brace) becomes popular in the seismic region such as Japan. It is anticipated to work as the energy dissipation device during earthquakes.

As illustrated in Fig.1.1, the frame where BRBs are installed into, is a truss structure (called as the BRB frame hereafter). Therefore the beams to which BRBs are connected, are subjected to axial force. However, the deformation capacity of beams is affected by the axial force. For example, when subjected to compression, strength degradation due to local buckling might be more frequent than the beams without compression. Moreover, the bending strength itself is reduced by axial force. Therefore combination of axial force and bending moment should be considered in designing beams in the BRB frame.

On the other hand, rigid-floor diaphragm is often assumed in the structural model when conducting structural analysis of multi-story buildings. This assumption brings many advantages, for example, drastic reduction of DOFs and stabilization by that, simplification of beam design by ignorance of the bending moment around the weak axis, etc (Chopra 2010). However, axial deformation of beams is perfectly neglected in the rigid-floor model, thus the axial force on beams cannot be obtained by the analysis.

Therefore, when using rigid-floor model, the axial forces should be estimated applying some procedure. In the present study, a simple scheme to estimate the axial force on steel beams in the BRB frame, is proposed. The estimation accuracy is verified using FE models in which the floor and skeleton are separately modelled using shell and beam elements, respectively. The FE model is elastic except the stress of BRB. The material nonlinearity in the behaviour of concrete slab or stud connector is ignored in the present study.

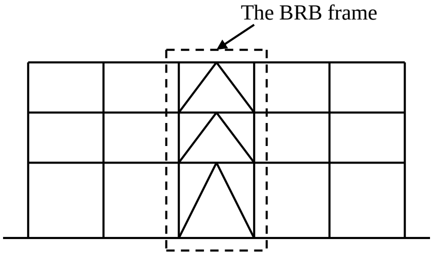


**Fig.1.1.** The BRB frame

## 2. ESTIMATION OF AXIAL FORCE

### 2.1 Axial force on composite beams

The beams contained in the BRB frame are assumed to be slab-composite beam. As illustrated in Fig.2.1, neglecting the shear force of columns, the inertia force acting on the BRB frame through the slab is equal to the difference between the horizontal component of BRBs stress in the *i*-th and *i+1*-th story.

$$P^i = \left(\left|N_{dL}{}^{i}\right| + \left|N_{dR}{}^{i}\right|\right)\cos\theta^i - \left(\left|N_{dL}{}^{i+1}\right| + \left|N_{dR}{}^{i+1}\right|\right)\cos\theta^{i+1} \tag{2.1}$$

where $P^i$ is the horizontal inertia force including inertia acting on the BRB frame that comes through the *i*-th floor. $N_{dL}{}^{i}$、 $N_{dR}{}^{i}$、 $N_{dL}{}^{i+1}$ and $N_{dR}{}^{i+1}$ are the axial forces of the BRBs in the *i*-th and *i+1*-th story.

An assumption, that $P^i$, the inertia force, acts to the BRB frame separately from left and right, is introduced. The left and right components of $P^i$, $P_L{}^i$ and $P_R{}^i$, are determined by Eq.(2.2).

$$\begin{aligned} P_L{}^i &= \alpha_L P^i \\ P_R{}^i &= \alpha_R P^i \end{aligned} \tag{2.2}$$

$\alpha_L$ and $\alpha_R$ represent the distribution ratio ($\alpha_L$ + $\alpha_R$ =1). The location on floor plan of the BRB frame affects the value of $\alpha_L$ and $\alpha_R$. Figs.2.2 show the simplest examples. $\alpha_L$ =0.05、 $\alpha_R$ =0.95 are assumed for the case shown in Fig.2.2(a) and $\alpha_L$ =$\alpha_R$=0.5 for the case shown in Fig.2.2(b). To determine the ratios of $\alpha_L$ and $\alpha_R$ at more complicated cases, further investigation is required.

Once $\alpha_L$ and $\alpha_R$ are determined, the axial forces of the composite beams in the BRB frame, are estimated using Eqs.(2.3). This is for the case when the BRBs are installed in reverse V shape;

$$\begin{aligned} N_{cbL}{}^{i} &= \mp\left(N_{dL}{}^{i+1}\cos\theta^{i+1} + P_L{}^{i}\right) \\ N_{cbR}{}^{i} &= \pm\left(N_{dR}{}^{i+1}\cos\theta^{i+1} + P_R{}^{i}\right) \end{aligned} \tag{2.3}$$

in which $N_{cbL}{}^{i}$, $N_{cbR}{}^{i}$ are the axial forces of the left and right composite beams in the *i*-th floor. The double sign represents the loading direction. The upper sign corresponds to the load toward right and the lower sign does reverse.

### 2.2 Axial force on steel beams

*2.2.1 Effect of configuration of BRB frame on axial force of beams*

Neutral axis of composite beam locates above the center of steel beam section. Then the steel beam is subjected to axial force and bending simultaneously even if the composite beam is subjected to only bending (Fig.2.4).

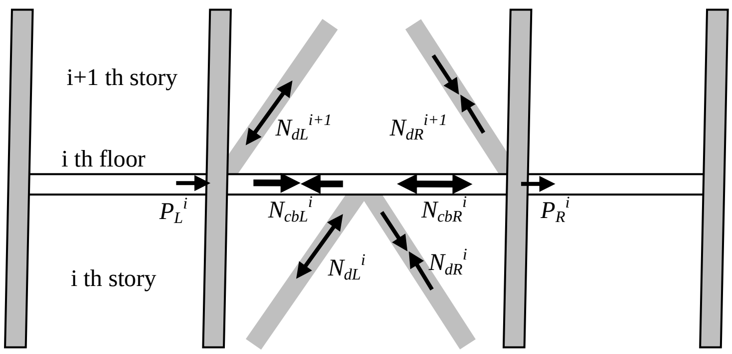


**Fig.2.1.** Equilibrium in the BRB frame

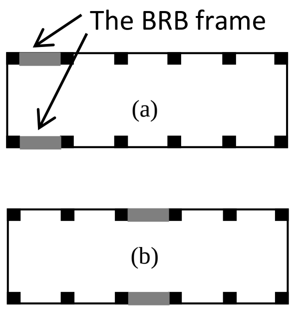


**Fig.2.2.** Location of the BRB frame

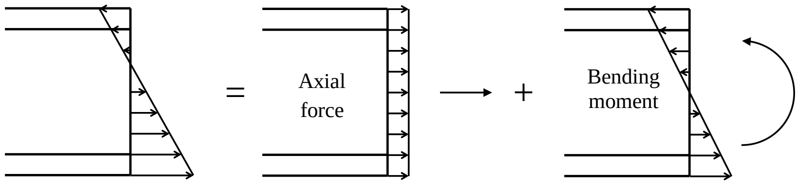


**Fig.2.4.** Combination of axial force and bending on steel beam

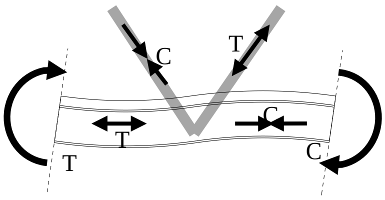


**Fig.2.5.** Stress in V-shaped BRB frame

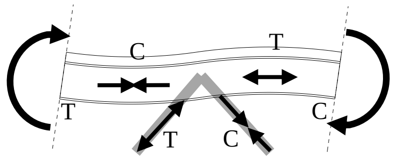


**Fig.2.6.** Stress in Reverse V-shaped BRB frame

The configuration of BRB frame effects on the axial forces of steel beams. When subjected to horizontal load toward right, the left end of steel beam is in tension due to bending on the composite section. When the configuration of BRB is V-shaped (Fig.2.5), the left beam is in tension due to the BRB forces. Therefore these two tensions act together on the steel beam. On the contrary, the stress on slab decreases by this stress superposition. When subjected to load toward left, the stress becomes reverse but this stress superposition is same.

When the configuration of BRB is reverse-V-shaped (Fig.2.6), the BRB forces yield the beam axial forces reverse to those due to bending. Therefore the axial forces of steel beams become smaller than those without BRB. But the stress of slab becomes larger.

*2.2.2 Estimation of axial force on steel beams*

The AIJ recommendation (the AIJ 2010) provides an explanation on section analysis of composite beams subjected to bending. Referring to the recommendation, a simple form to estimate the axial force on steel beam in composite section is derived herein. The composite section is subjected to both bending and axial force.

As indicated in Fig.2.7, an equilibrium among the axial forces (tension positive) holds.

$$N_{cb} = N_{sb} + N_{sl} \tag{2.4}$$

where $N_{cb}$, $N_{sb}$ and $N_{sl}$ are the axial forces on the composite section, steel beam section and floor slab, respectively. The suffices to represent the location of composite beam $_{L,R}$ and $^{i}$ are omitted. The bending moment on composite beam section (denoted by $M_{cb}$) is expressed in terms of $N_{sb}$, $N_{sl}$ and $M_{sb}$. $M_{sb}$ is the bending moment on the steel beam section.

$$M_{cb} = M_{sb} + N_{sb} j_{sb} - N_{sl} j_{sl} \tag{2.5}$$

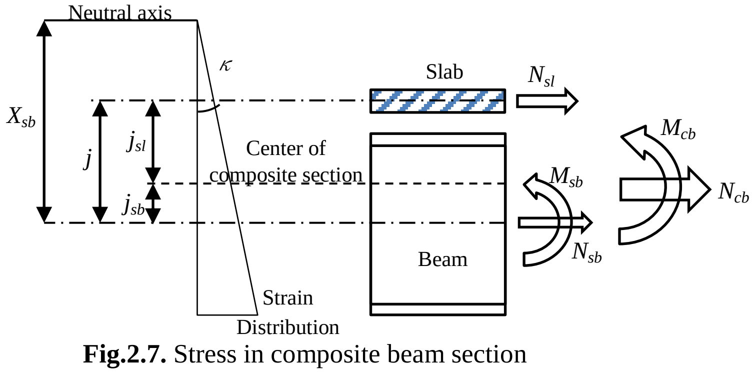


**Fig.2.7.** Stress in composite beam section

where $j_{sb}$ and $j_{sl}$ are the distance between the centers of composite and steel sections, composite and slab, respectively. Assuming elasticity, Eqs(2.4) and (2.5) are replaced into a simultaneous equation.

$$N_{cb} = \left\{ \left( EA_{sb} - \frac{EA_{sl}}{n} \right) X_{sb} - \frac{EA_{sl}}{n} j \right\} \kappa$$
$$M_{cb} = \left\{ EI_{sb} + \frac{EA_{sl}}{n} j \cdot j_{sb} + \left( EA_{sb} j_{sb} - \frac{EA_{sl}}{n} j_{sl} \right) X_{sb} \right\} \kappa \tag{2.6}$$

where $E$ represents the Young's modulus of steel. $I_{sb}$ and $A_{sb}$ are the second moment of inertia and area of the steel beam section. $A_{sb}$ and $n$ represents the area of slab and the Young's modulus ratio of steel to concrete. When determining $A_{sb}$, an effective width of slab is required. It is determined according to the AIJ recommendation. $j$ is the distance between the center of steel beam and slab. $\kappa$ represents the curvature of composite beam. By solving Eqs.(2.6), $X_{sb}$ is obtained.

$$X_{sb} = \frac{k_2}{k_1} \tag{2.7}$$
$$k_1 = M_{cb} \left( EA_{sb} + \frac{EA_{sl}}{n} \right) - N_{cb} \left( EA_{sb} j_{sb} - \frac{EA_{sl}}{n} j_{sl} \right), \quad k_2 = M_{cb} \frac{EA_{sl}}{n} j + N_{cb} \left( EI_{sb} + \frac{EA_{sl}}{n} j \cdot j_{sl} \right)$$

By substituting $X_{sb}$ into Eqs.(2.6) again, $\kappa$ is calculated. Then $N_{sb}$ is calculated using Eq.(2.8).

$$N_{sb} = EA_{sb} X_{sb} \kappa \tag{2.8}$$

When the deformation and stress in composite beam are small enough to assume elastic behavior, one can estimate the axial force on steel beam using Eq.(2.8) , from the axial force and bending moment on the composite beam.

## 3. VERIFICATION BY FE-ANALYSIS

### 3.1 Verification using one-way FE model (Model 1)

#### *3.1.1 FE-Model*

Using an FE model in which the slab and beam is separately modeled, the precision of estimated axial force is verified. At first, a one-way model (called as the "Model 1" hereafter, see Fig.3.1) is employed. This is a portion of a 3-storey building. The overview on the whole building is given in Fig.3.2 and Table 3.1.

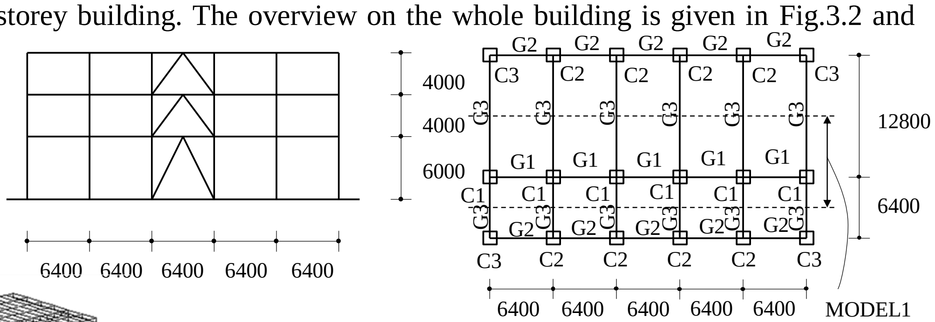


**Fig.3.2.** Model building

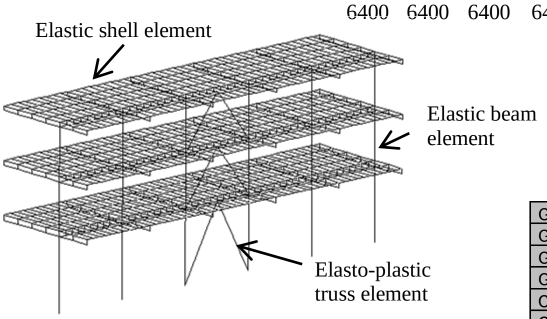


**Fig.3.1.** Model 1

**Table 3.1.** Section

| | 4F | 3F | 2F |
|---|---|---|---|
| G1 | H-550x250x9x19 | H-600x250x12x22 | H-650x250x12x25 |
| G2 | H-550x250x9x19 | H-600x250x12x22 | H-650x250x12x22 |
| G3 | H-550x200x12x22 | H-600x200x12x25 | H-650x200x12x25 |
| G4 | H-700x250x12x22 | H-750x250x14x25 | H-800x250x14x25 |
| C1 | □-450x450x19 | □-450x450x22 | □-500x500x22 |
| C2 | □-400x400x19 | □-450x450x19 | □-500x500x19 |
| C3 | □-350x350x16 | □-400x400x19 | □-400x400x19 |

The used FE software is MARC 2010 (MSC 2010). Elastic beam element is used for the model of column and beam. The panel zone is neglected. 4-node elastic shell element is used for the model of floor slab. The beam and shell elements are connected by rigid bar. Fig.3.3 illustrates this modelling concept. The Young's moduli and Poisson's ratio of beam elements are $2.05\text{x}10^5$ N/mm$^2$ and 0.3. Those for the concrete slab are $2.05\text{x}10^4$ N/mm$^2$ and 0.15.

Static pushover analysis is carried out. An assumption that all the mass of building distributes on the floor slab is introduced. The distributed mass is 8kN/m$^2$ for the 1$^{st}$ and 2$^{nd}$ floor, and 10kN/m$^2$ for the 3$^{rd}$ floor. The horizontal inertia force modelling earthquake load is given for the distributed mass on the floors. The horizontal loads for each floor are determined according to the BSL of Japan (BSL 2007). It is given in terms of story shear force $Q^i$.

$$Q^i = Z \cdot R_t \cdot A^i \cdot C_o \cdot \sum W^i \tag{3.1}$$

in which $Z$ and $R_t$ are the seismic zone factor and vibration characteristic factor, respectively. 1.0 is given for the both herein. $C_o$ is the standard base-shear coefficient. $\Sigma W^i$ is the weight to be supported by the story. $A^i$ is the vertical distribution factor.

$$A^i = 1 + \left( \frac{1}{\sqrt{\alpha^i}} - \alpha^i \right) \frac{2T}{1+3T}, \quad \alpha^i = \frac{\sum W^i}{W_t} \tag{3.2}$$

in which $T$ is the 1$^{st}$ natural period calculated assuming $T$=0.03$h$ ($h$: the height). $W_t$ is total weight above ground. Only the BRB is modeled as inelastic truss element in which a bi-linear force-deformation relation (Fig.3.4) is assumed. The yield force of the BRB is determined by Eq.(3.3).

$$N_{dy}{}^i = \beta \cdot \frac{Q^i}{2\cos\theta^i} \tag{3.3}$$

in which two values, 0.3 and 0.6, are given for $\beta$. 1.0 is set to $C_o$ in the calculation of $Q^i$.

Three FE models where the location of BRB frame is varied are made (Fig.3.5), called as the "Model 1-a,1-b and 1-c", respectively. Fig.3.6 shows an example of analyzed stress distribution. The color of the floor slab represents the intensity of Von Mises' stress at the middle surface.

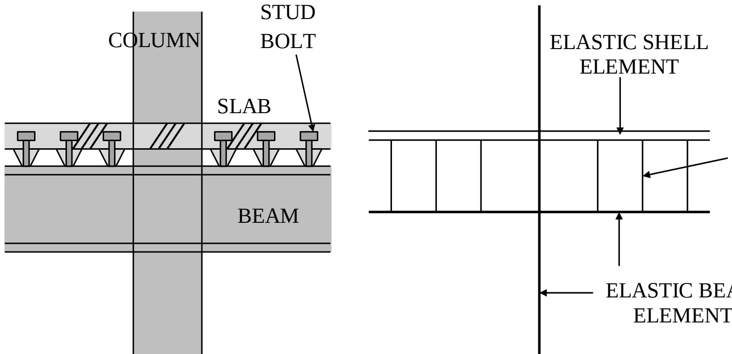


**Fig.3.3.** Modeling concept

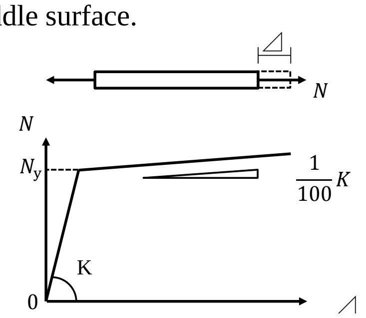


**Fig.3.4.** Force-deformation relation

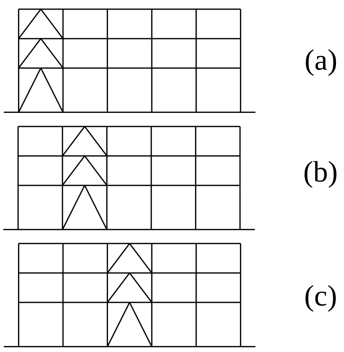


**Fig.3.5.** Three locations of BRB frame

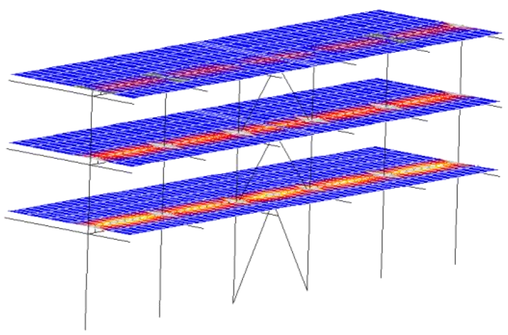

**Fig.3.6.** Stress distribution of Model 1-a

*3.1.2 Verification*

As for the Model 1, the axial forces on composite beams are calculated using the axial forces on floor slabs and steel beams directly obtained in the FE analysis. Fig.3.7 compares the estimated and obtained axial forces on the composite beams. In the estimation, Eq.(2.3) is applied where the combination of ($\alpha_L$ ,$\alpha_R$) are assumed to be (0.05,0.95) for the Model a, (0.25, 0.75) for the Model b and (0.5,0.5) for the Model c.

Good agreement between the analysis and estimation is observed. The estimation at $\beta$=0.6 is more close to the analysis than that at $\beta$=0.3. This is because the effect of shear force of column, neglected in the estimation, is relatively smaller.

## 3.2 Verification of estimated axial force on steel beam using rigid floor model

New two FE models for the whole structure of building shown in Fig.3.1 are constructed. One model is constructed assuming rigid-floor diaphragm (called the "Model 2" hereafter), which is ordinarily employed in structural design. The rigidity of composite beam is calculated according to the AIJ recommendation on composite structures (AIJ 2010).

The "Model 3" in which the slabs and beams are separately modeled, is constructed based on the same methodology as what is used in constructing the Model 1. Moreover, three models for each whole structure model are constructed (called as the Model 2-a,2-b 2-c, 3-a, 3-b and 3-c) where the location of BRB frame is varied like the Model 1. Figs.3.8 illustrates the Model 2-c and 3-c, for examples.

In the estimation procedure, firstly the axial force on the composite beams $N_{cb}$ is estimated using Eqs.(2.1)-(2.3). The combination of ($\alpha_L$ ,$\alpha_R$) are determined similarly to the Model 1. Then the axial force on steel beams are estimated using Eqs.(2.7) and (2.8). For $M_{cb}$, the bending moment on composite beam obtained in the analysis of the Model 2 is used.

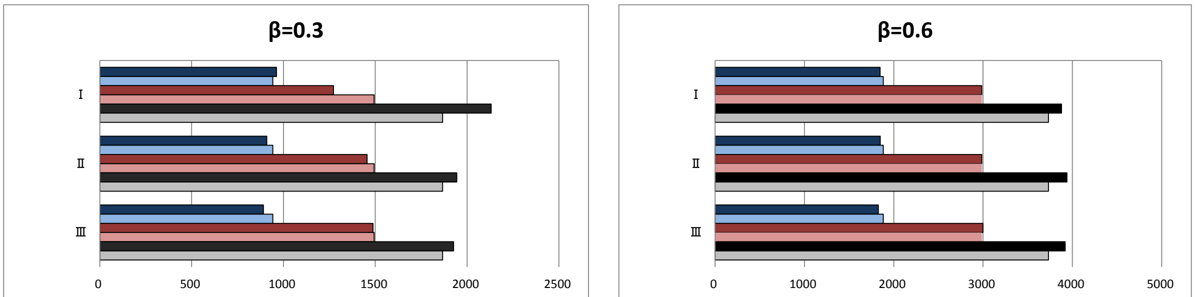


| UNIT:kN | III | II | I |
|---|---|---|---|
| 3F Analysis | 891 | 909 | 962 |
| 3F Estimate | 942 | 942 | 942 |
| 2F Analysis | 1487 | 1455 | 1272 |
| 2F Estimate | 1494 | 1494 | 1494 |
| 1F Analysis | 1927 | 1944 | 2131 |
| 1F Estimate | 1866 | 1866 | 1866 |

| UNIT:kN | III | II | I |
|---|---|---|---|
| 3F Analysis | 1828 | 1849 | 1848 |
| 3F Estimate | 1884 | 1884 | 1884 |
| 2F Analysis | 3000 | 2984 | 2985 |
| 2F Estimate | 2987 | 2987 | 2987 |
| 1F Analysis | 3920 | 3938 | 3878 |
| 1F Estimate | 3733 | 3733 | 3733 |

**Figs.3.7.** Verification using Model 1

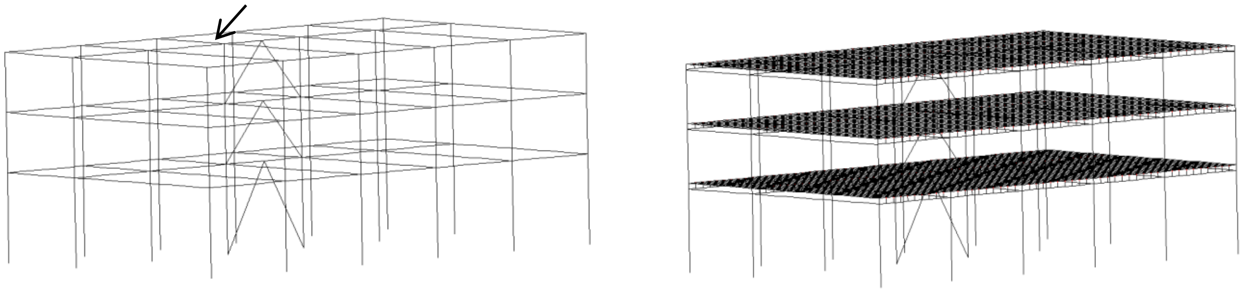


**Figs.3.8.** Model 2-c and 3-c

Figs.3.9 compares the estimated and analyzed axial forces on steel beams. The analyzed axial forces are obtained using the Model 3. The estimation error is larger than that of the one-way structure. It is considered to be due to the 2D extension of the stress distribution of slab. Moreover, errors when $\beta$=0.3 is relatively larger. It is considered to be due to the ignorance of column shear force when deriving Eqs.(2.1)-(2.3).

## 4. CONCLUSIONS

In the present paper, a simple scheme to estimate the axial force of steel beams in the BRB frame, is demonstrated. In the procedure, axial force on composite beams is estimated using Eqs.(2.1) to (2.3).

To calculate the axial force on steel section using Eqs (2.7) and (2.8), the bending moment on composite beam is required as well as the axial force. Rigid-floor model in which the beam is modeled as composite beam can provide the bending moment.

Verification using some FE models where the slabs and beams are individually modeled. As for the present models, the estimated axial forces show good agreement to the analyzed values.

However, the FE models might be too simple. In actual construction, many nonlinear factors, such as yield of skeleton, material strength of concrete slab, yield of stud bolt or contact and friction between column and slab, exist. Therefore use of more detailed nonlinear model is required.

**AKCNOWLEDGEMENT**

The authors express their gratitude for the Urban Disaster Mitigation Center of Kogakuin University for supporting the present research.

**REFERENCES**

Chopra, A. K. (2010). *Dynamics of Structures Theory and Application to Earthquake Engineering Third Edition.* Pearson-Prentice Hall. 2010

The Architectural Institute of Japan (2010). *Design Recommendation for Composite Constructions.* The Architectural Institute of Japan . 2010

The Building Standard Law of Japan (2007) The building centre of Japan. 2007

MSC Software (2010). *Marc 2010 Theory and User Information.* 2010

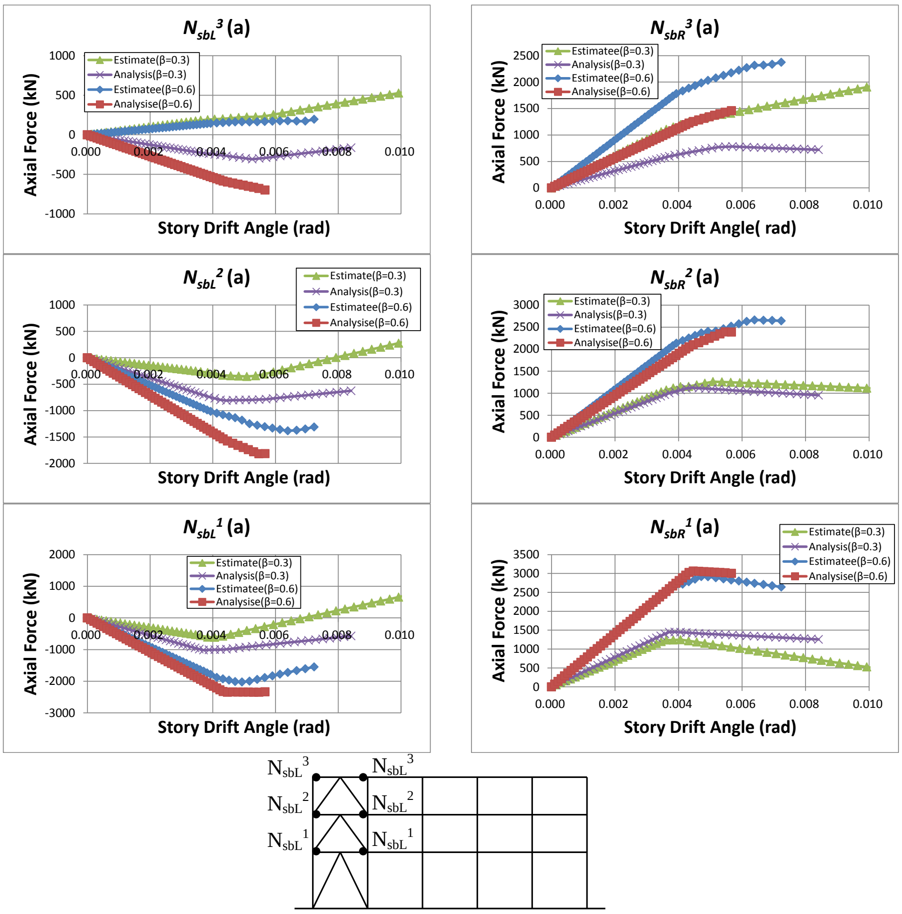

NsbL3 (a)
Estimate(β=0.3)
Analysis(β=0.3)
Estimatee(β=0.6)
Analysise(β=0.6)
Axial Force (kN)
Story Drift Angle (rad)
NsbR3 (a)
Story Drift Angle( rad)
NsbL2 (a)
NsbR2 (a)
NsbL1 (a)
NsbR1 (a)
NsbL3
NsbL2
NsbL1


(a)

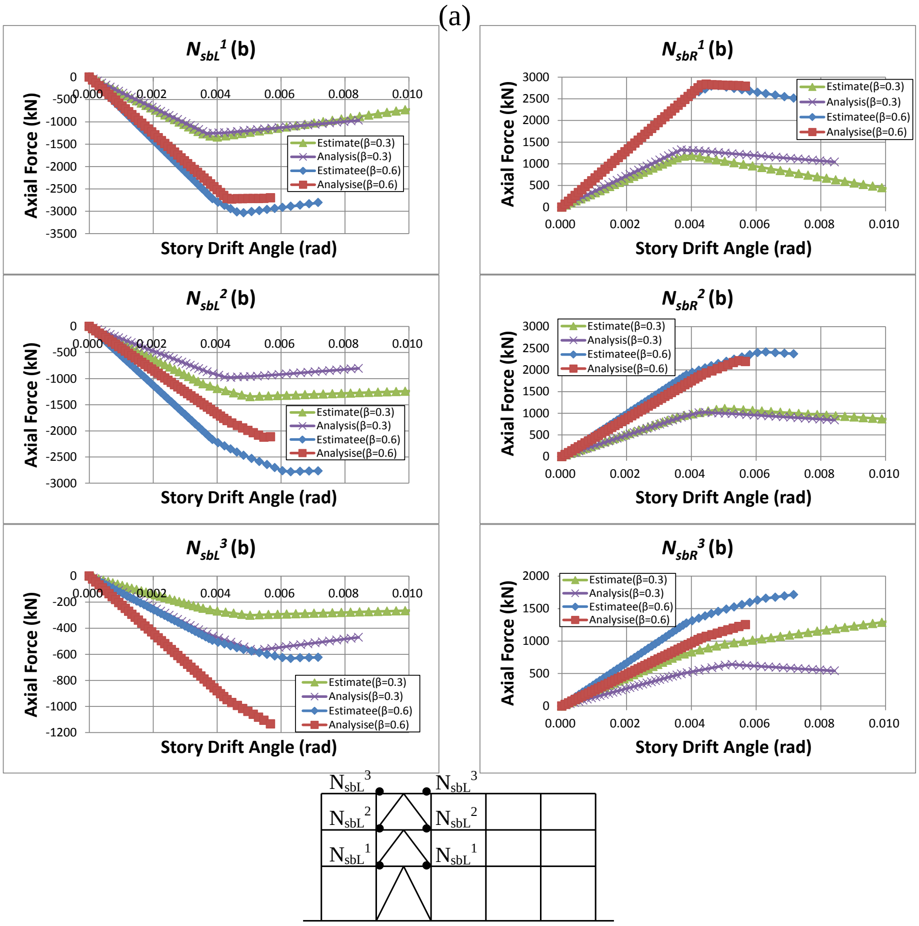

NsbL1 (b)
NsbR1 (b)
NsbL2 (b)
NsbR2 (b)
NsbL3 (b)
NsbR3 (b)
Estimate(β=0.3)
Analysis(β=0.3)
Estimatee(β=0.6)
Analysise(β=0.6)
Axial Force (kN)
Story Drift Angle (rad)
NsbL3
NsbL2
NsbL1


(b)

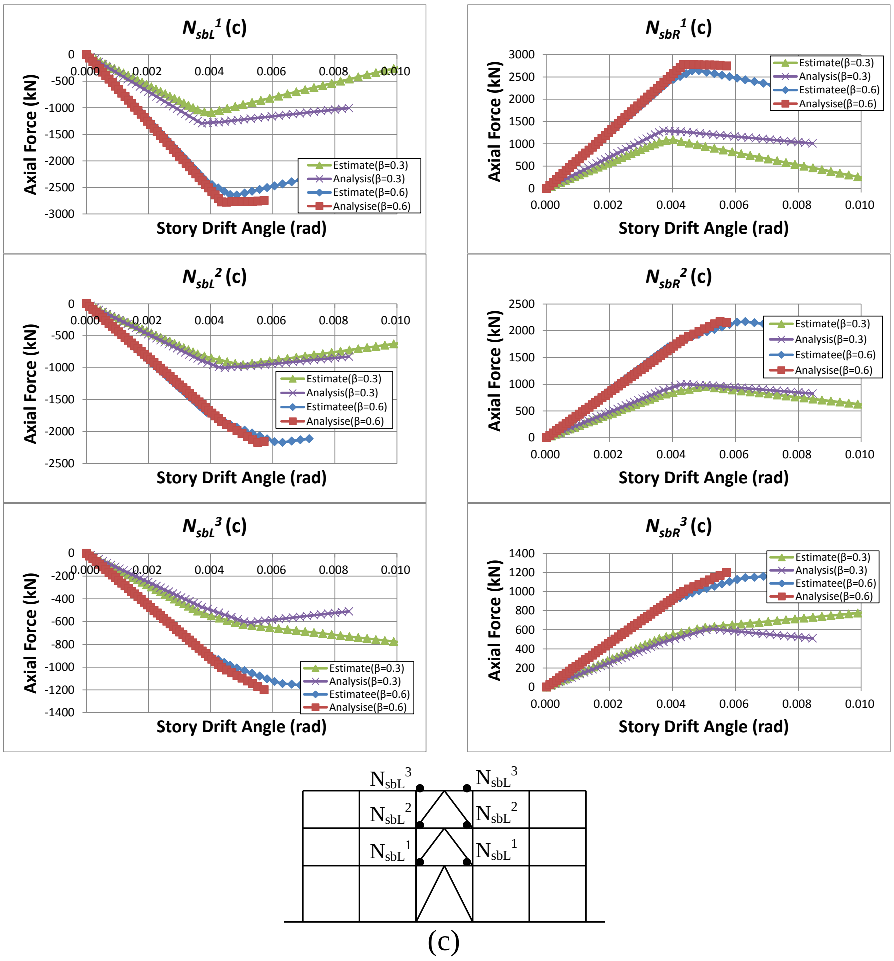


**Figs.3.9.** Comparison between estimated and analyzed axial forces